A new integrated single-chamber air-cathode microbial fuel cell - anaerobic membrane bioreactor system for improving methane production and membrane fouling mitigation

Yuankun Hao[a, b], Xinbo Zhang[a, b, d*], Qing Du[a, b], Huizhong Wang[a,b], Huu Hao Ngo[a, c*], Wenshan Guo[a, c], Yufeng Zhang[a,b], Tianwei Long[a,b], Li Qi[a,b]

[a] *Joint Research Centre for Protective Infrastructure Technology and Environmental Green Bioprocess, School of Environmental and Municipal Engineering, Tianjin Chengjian University, Tianjin 300384, China*

[b] *Tianjin Key Laboratory of Aquatic Science and Technology, Tianjin Chengjian University, Jinjing Road 26, Tianjin 300384, China*

[c] *Centre for Technology in Water and Wastewater, School of Civil and Environmental Engineering, University of Technology Sydney, Sydney, NSW 2007, Australia*

[d] *School of Chemistry and Materials Science, University of Science and Technology of China, Hefei, Anhui, 230026, China*

*Correspondence authors: Email: zxbcj2006@126.com (X. B. Zhang); ngohuuhao121@gmail.com (H. H. Ngo)

Abstract

A novel integrated single-chamber air-cathode microbial fuel cell - anaerobic membrane bioreactor (ScMFC-AnMBR) system was designed. It involved an anaerobic membrane bioreactor (AnMBR) and a single-chamber air-cathode microbial fuel cell (ScMFC) being constructed in a common reaction chamber to enhance methane production and reduce membrane fouling in the AnMBR. Results indicated that ScMFC-AnMBR delivered a stable micro-bioelectric field environment with a voltage output of 95±4 mV. Compared with conventional AnMBR (C-AnMBR), methane production using this system increased by 35.89%. Soluble microbial product (SMP) and extracellular polymeric substances (EPS) dropped by 65.3% and 43.1%, respectively. Particularly, the transmembrane pressure (TMP) in the operating cycle was in a slow growth status with the maximum value of only 18.5 kPa. The bioelectric field helped aceticlastic methanogens (*Methanosaeta*) replace hydrogenotrophic methanogens (*Methanobacterium*) as the dominant methanogens via electron transfer under a closed-circuit scenario. As syntrophic bacteria of methanogens (*Syntrophobacter*, *Smithella* and *Syner-01*) and exoelectrogens of *Desulfovibrio* were selected by the bioelectric field and gained a stable foothold, bio-foulant (*Megasphaera*) was significantly reduced. The complex microbial synergism in ScMFC-AnMBR greatly improved the methanogenic performance, thus effectively alleviated membrane fouling and prolonged the operation cycle of the system. Demonstrated here is the feasibility of practical application.

Keywords Bioelectric field; Single-chamber air-cathode microbial fuel cell; Anaerobic membrane bioreactor; Methane production; Membrane fouling

1. Introduction

An efficient wastewater treatment strategy is very important for maintaining clean water supplies. Aerobic wastewater treatment technology has been in use for than a century, yet the advantages of wastewater reuse waned due to its high energy consumption and huge greenhouse biogas emissions [1]. Compared with aerobic technologies the, anaerobic membrane bioreactor (AnMBR) process stands out based on its advantages of low energy consumption, small footprint, small sludge yield, production of recyclable biogas, etc. [2]. In recent years, many large-scale and pilot-scale AnMBRs have been conducted for the treatment of high-concentration industrial wastewater and low-concentration domestic wastewater.

Although AnMBRs produce good effluent quality, membrane fouling is still an important problem in their application. Membrane fouling can reduce flux, shorten membrane life and increase cleaning frequency, thus reducing the economical aspect of membrane filtration. Compared with aerobic sludge, anaerobic sludge has higher tendency to produce particles, which results in more serious and irreversible membrane fouling [3]. The mechanism that leads to membrane fouling is very complex. Studies suggested that such fouling mainly consists of pore clogging, formation of soluble microbial products (SMPs), extracellular polymeric substances (EPSs) and mud cake layer. Many pollutants such as particles of a large size and microorganisms exist in the liquid feeding matrix of AnMBRs. Small particle-sized particles may enter the interior of the membrane assembly and cause blockages, while those of large particle size may attach to the surface of the membrane assembly and form a dense mud cake layer [4, 5]. The high intensity interaction between pollutants (such as SMPs and EPSs) and the membrane leads to a blockage of membrane pores and the formation of a mud cake layer. Wang, Bi, Ngo, Guo, Jia, Zhang and Zhang [6] pointed out that EPS and SMP are negatively charged, so the electrochemical environment will effectively alleviate the deposition of fouling on the membrane components.

To control membrane fouling, many researchers have introduced the electric field concept into AnMBRs. Katuri, Werner, Jimenez-Sandoval, Chen, Jeon, Logan, Lai, Arny and Saikaly [7] applied a small voltage of 0.7 V to the AnMBR, and their results showed that membrane fouling was effectively alleviated, and pointed out that increasing methane production might be linked to this electric field environment. A MEC-AnMBR reactor with an applied voltage of 0.6 V was constructed by Ding, Fan, Cheng, Sun, Zhang and Wu [8] and the results showed that the operational period of the membrane was 1.63-fold times larger than the original. Yang, Qiao, Jin, Zhou and Quan [9], [10] applied a carbon nanotube-based hollow fiber conductive membrane in AnMBR, and discovered that membrane fouling could be effectively mediated at an applied small voltage of 1.2 V. In an electro-AnMBR system constructed by Zhang, Yang, Liu, Xu, Hei, Zhang, Chen, Zhu, Liang, Zhang and Huang [11] with the applied voltage reduced to 0.5 V, results showed that the membrane fouling rate and substances dropped by 23% and 10%, respectively. Previous studies proved that the existence of a micro electric field can effectively alleviate membrane fouling, but the applied electric field still consumed a lot of energy. Consequently, it is necessary to find a more energy-saving and effective method to prevent or minimize membrane fouling.

Microbial fuel cells (MFCs) can directly convert organic matter into useful electrical energy through redox reactions catalyzed by microorganisms, which is a new wastewater treatment technology and can reduce the net energy requirement in pollutants treatment. In recent years, great progress has been made in optimizing the structure, operating conditions, and synthesizing electrode materials of MFC. Technologies that combine MFC with other wastewater treatment processes have attracted wide attention. For instance, the combined reactor of MFC and AnMBR as devised by Tian, Ji, Wang and Le-Clech [12] for the first time treated domestic wastewater, with nitrate nitrogen wastewater the influent of MFC cathode chamber and nitrate nitrogen as electron acceptor. The outcomes showed that membrane fouling diminished by 11.3%. Evidence demonstrated that MFC (0.1 V of cell potential) combined with AnMBR showed that the bioelectric field could effectively alleviate membrane fouling in a more energy-saving way utilizing only 0.52%–0.99% of electric energy [13]. Recently, Yang, Wang, Zhang, Jia, Zhang and Gao [14] constructed a single-chamber MFC to reinforce anaerobic digestion, and the existence of a bioelectric field enhanced anaerobic digestion, achieving significantly higher COD removal efficiency (86%) and biogas production (240 ml/d). Such research fully revealed that the MFC can alleviate membrane fouling of AnMBR to a certain extent, and even improve its performance.

However, the MFC-AnMBR system in current research is a combination process, rather than a real coupling system, which has the limitation of producing a large footprint. The combined processes of MFC and AnMBR ignore the synergistic effect of microorganisms in the two reactors. The underlying mechanism for the membrane fouling mitigation and changing the performance of AnMBR in the bioelectric field are still unclear, and must be further explored. Thus, in this work, a novel integrated single-chamber air-cathode microbial fuel cell - anaerobic membrane bioreactor (ScMFC-AnMBR) system was designed by involving an anaerobic membrane bioreactor (AnMBR) and a single-chamber air-cathode microbial fuel cell (ScMFC) in a common reaction chamber to enhance methane production and reduce membrane fouling in the AnMBR. The chemical oxygen demand (COD) removal, methane production, membrane fouling and microbial community structure of the ScMFC-AnMBR were examined and compared with that of conventional AnMBR (C-AnMBR) system at the same operating conditions. The characteristics of AnMBR performance and the mechanism of membrane fouling mitigation in the bioelectric field were further assessed. This can contribute to the feasibility of AnMBR-based technology in practical applications and provide technical support for large-scale and low-cost wastewater treatment strategies.

2. Materials and Methods

2.1 Integrated ScMFC–AnMBR system

The ScMFC-AnMBR system consists of an AnMBR and single chamber air cathode MFC, as shown in Fig. 1. The two systems share a reactor (a height of 30.5 cm, and a bottom circle diameter of 10 cm) with an effective volume of 2.0 L. An anaerobic membrane bioreactor acts as the MFC anode chamber, and the anode electrode (carbon felt with a size of 5×8 cm and effective area of 40 cm^2) and membrane components were placed inside. The direct current (DC) resistance box (ZX21, Shanghai Dongmao Technology Co., Ltd.) was connected to a copper wire between the electrodes of the bipolar chamber. Cell voltages were collected every 10 min by connecting a data acquisition card (DAM-3000m, Beijing Altai Technology Co., Ltd.). C-AnMBR served as the control. YZ1515X peristaltic pumps work as water inlet and outlet devices. The circulating constant temperature water bath device (Wuxi Billang Experimental Instrument Manufacturing Co., Ltd.) helped to maintain the temperature of ScMFC-

AnMBR and C-AnMBR. The biogas produced by anaerobic digestion was collected by aluminum foil biogas collection bags. According to Jeong, Kim, Jin, Hong and Park [15], ScMFC-AnMBR used a self-circulation device of biogas generation to replace the traditional stirring device. The self-circulation process of biogas was that when it is generated in the anaerobic digestion process, the biogas enters the pumping dual-purpose vacuum pump (D50 remote control type (Chengdu Hailin Technology Co., Ltd.). It does this through the buffer bottle and drying bottle, and then enters the aeration disc in the reactor through the biogas flowmeter (LZB-3WB type), replacing the mixing device to achieve the purpose of mud and water mixing. Both systems were operating under dark conditions.

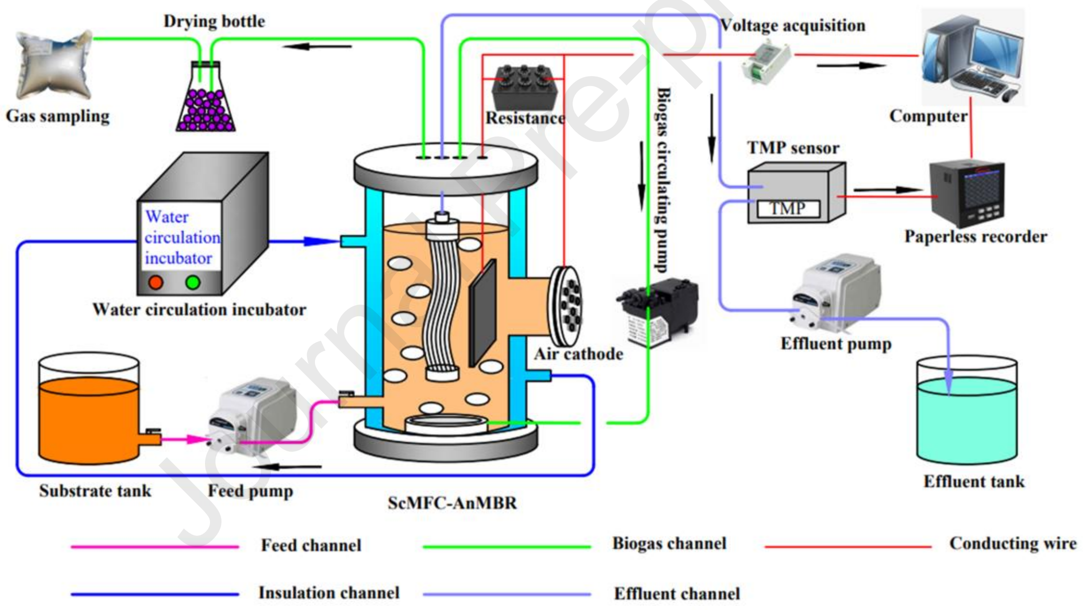

Fig. 1. Schematic diagram of the ScMFC-AnMBR system

2.2 Experimental materials and operating conditions

Membrane components of both systems adopted polyvinylidene fluoride (PVDF) hollow fiber membrane (aperture 0.1 μm, Guangzhou Haike Membrane Technology Co., Ltd.), and the effective filtration area was 0.042 m^2. The transmembrane pressure values of the two reactors were recorded by paperless recorder (MIK-R9600, Hangzhou Meikong Automation Technology Co., Ltd.). The pretreatment steps were as follows:

the carbon felt was soaked in 1 mol·L^{-1} HCl and 1 mol·L^{-1} NaOH for 24 hours respectively, and then dried for later use. The materials required for the preparation of air cathode are non-woven carbon cloth, poly tetra fluoroethylene (PTFE) emulsion, carbon black, platinum carbon, nafion 20% membrane solution (Shanghai Hesen Electric Co., Ltd.), isopropyl alcohol. The air cathode production method was implemented based on what other research suggested [16].

Synthetic wastewater with a ratio of 205:5:1 of C: N: P was used in the experiment. The essential components of wastewater contained $C_6H_{12}O_6$ (3000 mg·L^{-1}), NH_4Cl (120 mg·L^{-1}), KH_2PO_4 (120 mg·L^{-1}), $MgSO_4$ (30 mg·L^{-1}), and $FeCl_2$ (112 mg·L^{-1}). The essential trace elements included $MnCl_2$ (1 mg·L^{-1}), $ZnCl_2$ (1 mg·L^{-1}), $NiCl_2$, (21 mg·L^{-1}), $CoCl_2$ (13 mg·L^{-1}), $CuCl_2$ (0.25 mg·L^{-1}), H_3BO_3 (0.05 mg·L^{-1}), and Na_2MoO_4 (0.24 mg·L^{-1}). The composition of phosphate buffer solution (PBS) buffer was made up of Na_2HPO_4 (4.58 g·L^{-1}), and NaH_2PO_4 (2.13 g·L^{-1}).

The inoculated sludge was collected from the anaerobic digestion tank of a sewage treatment plant in Tianjin, and the mixed liquor suspended solids (MLSS) of inoculated sludge was 40000 mg·L^{-1}. 500 mL inoculated sludge was added into the anode chamber of ScMFC–AnMBR and C-AnMBR, respectively. The circulating constant temperature water bath system was set outside the two systems devices to ensure that the temperature in the two systems remained stable at 35 °C. PBS buffer was added to obtain the pH in the two reactors and it was stable between 6.5 and 7.5. The dissolved oxygen in the two reactors was controlled below 0.2 mg·L^{-1} to ensure a strict anaerobic environment. The self-circulation system controlled the aeration rate through a timing switch, and the circulating aeration rate of the two reactors was stable at 0.8 L·h^{-1}.

Both systems had the same influent load and adopted intermittent influent followed by continuous influent. The influent concentration increased step-by-step in three gradients. During Stage I (day 1), influent COD concentration was 0 mg·L^{-1}, and the operation at this influent concentration lasted only one day to complete the sludge standing. At Stage II (days 2 to 35), the influent COD concentration rose to 1590 mg·L^{-1}, and ScMFC-AnMBR was regarded as successful when the voltage peak reaches 100 mV for 12 consecutive days at this influent concentration. At this time, the influent mode changed from intermittent influent to continuous influent. For Stage III (days 36 to 75), based on the premise of successful start-up of ScMFC-AnMBR, the influent COD concentration increased to 3180 mg·L^{-1} when the COD removal of both systems reached 80%. Hydraulic retention time (HRT) stabilized at 96 h.

2.3 Analysis methods

During the operation, the pH of sludge mixture in the two reactors was determined by pH portable tester (HACH HQ11D, USA), while COD was detected by potassium dichromate rapid digestion spectrophotometry. MLSS and mixed liquid volatile suspended solids (MLVSS) were measured using the gravimetric method [17]. SMP was extracted by the centrifugal-filtration method, EPS was further separated from the sludge mixture via the pyrolysis method. The carbohydrate in SMP and EPS was measured by phenol-sulfuric acid method, and the protein was measured employing the Folin–Ciocalteu method [18]. The fluorescence emission matrix spectra of SMP and EPS were measured by three-dimensional fluorescence spectrophotometer. Sludge particle size was determined by Malvern laser particle size analyzer (Malvern Masters Sizer 2000, Malvern Instruments, UK).

Zeta potential analyzer measured the surface charge of sludge. Volatile fatty acids (VFAs) were determined by biogas chromatograph (PerkinElmerClarus, USA). For ScMFC-AnMBR, electrochemical potentiostat (Shanghai Chenhua Instrument Co., Ltd.) measured the cyclic voltammetry curves. After successful start-up, the polarization curve of ScMFC-AnMBR was analyzed by the steady-state discharge method, wherein the curve of voltage and power density changing with current density was obtained by adjusting the change of resistance value of external resistance. The coulomb efficiency (CE) [1] was calculated by combining COD removal, resistance value and voltage value of ScMFC-AnMBR. The actual electron recovery rate of substrate and theoretical electricity generation under the actual substrate concentration could be obtained, and the calculation formula is written as follows (1):

$$CE = {}^{32\sum_{i=1}^{n} U_i t_i} / _{RFbV\Delta COD} \quad (1)$$

where: U denotes the voltage output at t time; R is resistance value; F stands for Faraday constant (96485 C/mol); and b represents the number of electrons produced theoretically per consumption of 1 mol COD. High-throughput sequencing was done on the inoculated sludge and the sludge at the experiment's later stage in the two systems (commissioned by Shanghai Meiji Biomedical Technology Co., Ltd.). Refer to the research conducted by Chen, Zhang, Zhang, Ma, Liu, Cao, Chai and Chen [19] for specific steps.

3. Results and discussion

3.1 Electricity generation performance of the ScMFC-AnMBR integrated system

3.1.1 Voltage and Power density

The voltage and power density of ScMFC-AnMBR during the entire operating cycle (1800 h) are shown in Fig.2a and 2b. The ScMFC-AnMBR system was successfully started at 414 h, and the voltage output from it was stable at 107±14 mV in the following 456 hours (until Stage III commenced). Meanwhile, the maximum power density reached 342.23 $mW \cdot m^{-2}$. In Stage III (3180 $mg \cdot L^{-1}$ of the influent COD concentration), the voltage of ScMFC-AnMBR finally stabilized at 95±4 mV, and the maximum power density reached 225.63 $mW \cdot m^{-2}$. Although the complex flora in ScMFC-AnMBR easily caused a low relative abundance of exoelectrogens [20, 21], the tiny amount of bioelectric field obtained remained very stable throughout the operation cycle. Additionally, compared with ScMFC-AnMBR before and after the increase in the influent load, it was obvious that voltage and power density duplicated the trend of decreasing first and then stabilizing, and the power generation performance after stabilizing was less than before (voltage output and maximum power density decreased by 11.2% and 34.1%, respectively). This was because it taken some time for exoelectrogens to adapt to the impact brought about by the rising organic load, and there was no positive correlation between extracellular electron transfer and organic load [22].

In this study, AnMBR and ScMFC shared the same chamber, which involved the distribution of carbon sources. For this reason, it was speculated that the continuous and stable micro-bioelectric field changed the community structure of microorganisms, and the increase in the relative abundance of some non-exoelectrogens (such as methanogens) might allocate more carbon sources.

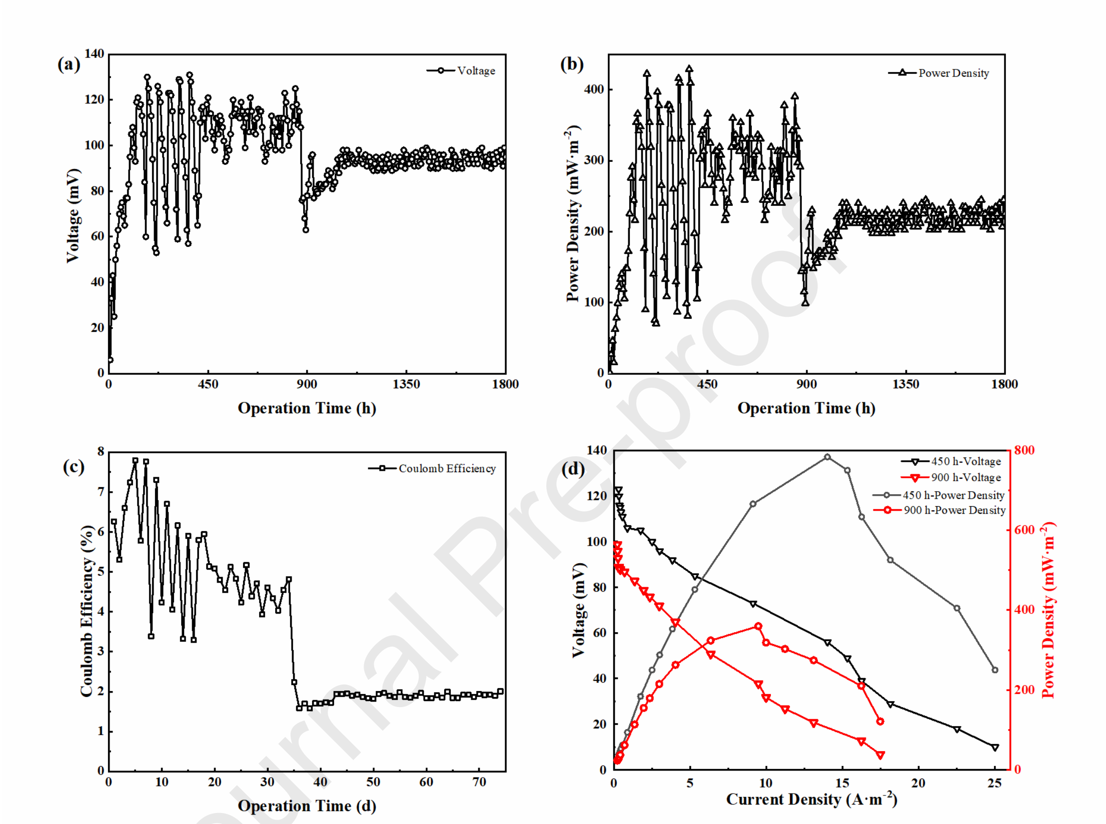

Fig. 2. Variations in (a) voltage output, (b) power density, (c) coulomb efficiency with time and (d) polarization curves of ScMFC–AnMBR at the initial successful start-up (450th hour) and when the influent load increases (900th hour).

3.1.2 Coulomb efficiency and polarization curve

As shown in Fig. 2c, coulomb efficiency of ScMFC–AnMBR was below 7.79% and not positively correlated with the influent load. It was speculated that since glucose can be used by a variety of non-exoelectrogens due to its special fermentation properties, so the CE obtained when glucose was used given the substrate was lower [23]. In addition, the power generated in the ScMFC-AnMBR did not increase when organic matter degradation improved, resulting in the coulomb efficiency falling to 1.9% later on during the experiment. This may be due to the increase of influent load, the rate of exoelectrogens in ScMFC-AnMBR to reproduce and metabolize and consume substrates for electron transfer reaches its peak at the same time, and the increase of non-exoelectrogens leads to a decrease in CE.

The polarization curve of ScMFC-AnMBR was measured at the initial stage of successful start-up (450th hour) and when the influent load was increased (900th hour) (Fig. 2d). It was very clearly observed that the power generation performance of ScMFC-AnMBR declined significantly after the influent load increased, peak values of power density obtained from the two measurements were 784 $mW \cdot m^{-2}$ and 361 $mW \cdot m^{-2}$, and the corresponding current densities were 14 $A \cdot m^{-2}$ and 9.5 $A \cdot m^{-2}$, respectively. A larger external resistance value (1000 Ω) was selected for ScMFC-AnMBR to maintain a stable low voltage output, which not only alleviated membrane fouling but also did not allocate too many carbon sources [24].

3.1.3 Cyclic voltammetry curve

The electron transfer between microbial or biofilm and MFC anode can be analyzed by using the cyclic voltammetry characteristic curve [25]. From the cyclic voltammetry curve of ScMFC-AnMBR at the later stage of the experiment (shown in Fig. S1), the cyclic voltammetry curve of ScMFC-AnMBR revealed no obvious redox peak while the integral area of scanning curve was small, indicating a uniform and poor charge/discharge capacity of ScMFC-AnMBR system. Discharge capacity can be used to characterize the stability of the ScMFC-AnMBR system's generation of power. The scanning curve of ScMFC-AnMBR did not change greatly when the scanning cycles increased, meaning that ScMFC-AnMBR remained stable when generating power and can meet the requirements of long-term operation.

3.2 Effect of the bioelectric field on the AnMBR performance

3.2.1 Wastewater treatment performance

The ScMFC-AnMBR and C-AnMBR's removal of COD during the operational period are shown in Fig. 3a. In Stage II (actual influent COD concentration of 1586.6±8.9 $mg \cdot L^{-1}$), the COD removal of both ScMFC-AnMBR and C-AnMBR did improve with the extension of operations. When the COD removal of C-AnMBR reached 80%, the COD removal of ScMFC-AnMBR reached as high as 98.61%. It was indicated that ScMFC-AnMBR removal of COD went up significantly faster, and the bioelectric field helped the AnMBR system to complete the rapid start. At the end of Stage II, the COD removal of ScMFC-AnMBR reached 99.33%, which was 1.2 times better than that of C-AnMBR. This was due to being under the same influent load, where the bioelectric field can help improve the activity of methanogens, consequently affecting the anaerobic digestion process [26].

In Stage III (the actual influent COD concentration increased to 3177.3±11 mg·L^{-1}), the COD removal of the two systems declined suddenly when the influent load increased. The COD removal of ScMFC-AnMBR and C-AnMBR decreased to 72.27% and 92.83%, respectively, whereas the trend still gradually rose. As in Stage II, the improvement in COD removal in ScMFC-AnMBR was still faster than that in C-AnMBR. At the end of Stage III, the COD removal of ScMFC-AnMBR reached 99.81%, significantly higher than that of C-AnMBR by 12.09%. With regard to the influent load increase, the ScMFC-AnMBR system – with the COD removal always above 90% - presented stronger tolerance than C-AnMBR. This was explained by the bioelectric field strengthened the electron transfer chain between microbial cells, enhanced the sludge activity and shortened the time for microbes to adapt to changes in the external conditions [27]. In addition, the organic load of wastewater treated in this experiment is much higher than that of domestic sewage (usually less than 500 mg·L^{-1}) so that the integrated system not only can meet the treatment needs of domestic sewage, but also treat high concentration organic wastewater in practical application.

To further gain an insight into the energy distribution of the ScMFC-AnMBR system during stable operation, the mass balances of COD were analyzed in stage III (the procedures for all calculations were listed in the Supplementary Materials) [6]. The influent COD concentration in stage III was 3177.3±11 mg·L^{-1}, and the permeate flux was maintained at 0.5 LMH. It was known that the TCOD in the influent was 1601.4 mg·d^{-1}. The average COD removal of ScMFC-AnMBR and C-AnMBR were 97.31% and 83.43% respectively in stage III, and the COD of the effluent (named Nd-COD) in the two systems were 43.1 mg·d^{-1} and 265.4 mg·d^{-1} respectively. Based on the average CE (1.91%) of ScMFC-AnMBR in stage III, it could be known that the COD used for electricity generation was 29.8 mg·d^{-1}. It can be inferred that 1.8% energy of the sewage in ScMFC-AnMBR was converted into electric energy. Although the power generation process in ScMFC-AnMBR accounted for a little part of COD consumption, the system could effectively recover energy from wastewater without external energy consumption.

3.2.2 Methanogenic performance

The methane production of ScMFC-AnMBR and C-AnMBR was measured to evaluate the two systems' production performance (Fig. 3b). The production in both systems increased with the extension of operational time, indicating the development of methanogens. At the beginning of Stage II, methane production and methane content in biogas production accounted for 6.99 mL·gCOD^{-1} and 22.26%, respectively, which were 65.1% and 86% of the C-AnMBR under the same influent load. It emerged that the methanogenic performance of ScMFC-AnMBR was not as good as that of C-AnMBR at the beginning. The enrichment activities of exoelectrogens resulted in a inhibited metabolic activity of methanogens at the initial start-up stage. Subsequently, in the middle and late stage of Stage II, the methane production of the ScMFC-AnMBR system was 38.89 mL·gCOD^{-1} and 67.84 mL·gCOD^{-1}, respectively, reaching 137.4% and 161.9% of that of C-AnMBR.

It was indicated that the rise rate of methane production of ScMFC-AnMBR was significantly faster than that of C-AnMBR. It was because direct electron transfer between species provided a better breeding environment for methanogens in ScMFC-AnMBR [28]. In the meantime, the exoelectrogens in ScMFC-AnMBR reached the peak value and tended to remain stable through the electron transfer of consuming substrates, so that the activity of methanogens would not be inhibited by the problem of substrate competition. The voltage output in this period was stable at 107±14 mV. Then in Stage III, the methane production of the two systems indicated a positive correlation with the influent load, while that of ScMFC-AnMBR increased faster. At the end of the whole operation time, the methane production of ScMFC-AnMBR and methane proportion in produced biogas reached 85.92 mL· gCOD^{-1} and 52.54%, respectively. They were all 1.2 times higher than C-AnMBR. This confirmed that the bioelectric field can enhance the activity of methanogens and consequently the methanogenic performance of the ScMFC-AnMBR system.

The concentration of VFAs can directly reflect the activity of methanogens in the reactor [29], so it is important to understand the operational status of the two systems by measuring the VFAs concentration (Fig. 3c and 3d). Clearly, the VFAs content in C-AnMBR was as high as 2778.37 $mg \cdot L^{-1}$ at the early stage of experimental operation, 7.2 times that of ScMFC-AnMBR. It emerged that serious acidification occurred in C-AnMBR, which was very unfavorable for commencing the AnMBR system, because the high content of VFAs inhibited the reproduction of methanogens and degradation of organic matter [30]. However, the existence of the bioelectric field improved the VFAs utilization rate and shortened the start-up period of ScMFC-AnMBR system. It is one reason why the COD removal of ScMFC-AnMBR rose much faster than that of C-AnMBR in the early stages of the experiment.

Although the VFAs content in C-AnMBR decreased to 626.35 $mg \cdot L^{-1}$ at the end of operation, it was still 2.6 times higher than in ScMFC-AnMBR. It was consistent with the optimization of organic degradation and methanogenic performance of ScMFC-AnMBR. At the same time, acetic acid was undetected in ScMFC-AnMBR, indicating that the anaerobic digestion process in ScMFC-AnMBR was smoother, presumably due to the existence of a bioelectric field enhancing the activity of aceticlastic methanogens. As well, the propionic acid content, considered to be highly toxic, was significantly smaller in ScMFC-AnMBR compared to the C-AnMBR. It also indicated the stronger activity of methanogens in ScMFC-AnMBR.

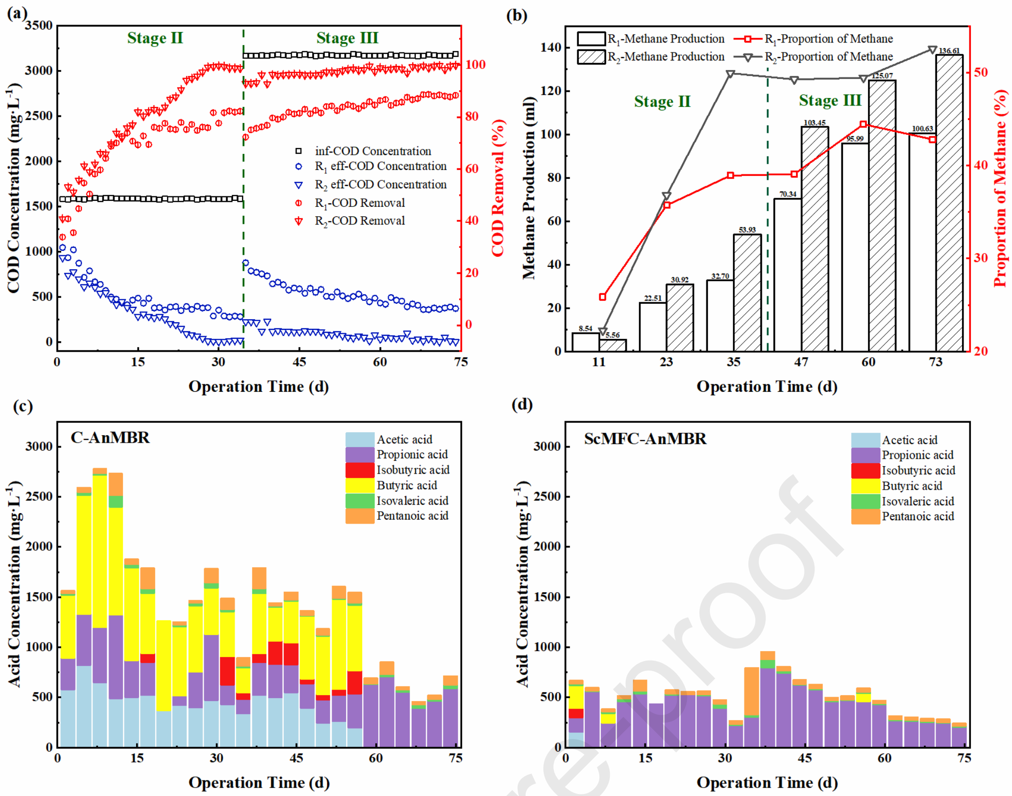

Fig. 3. Variation of (a) COD removal, (b) methane content, volatile fatty acid content in (c) C-AnMBR (R_1) and (d) ScMFC-AnMBR system (R_2) with time. inf-COD: influent COD concentration; eff-COD: effluent COD concentration.

3.2.3 Sludge characteristics

The optimum pH range for methanogens ranges from 6.8 to 7.2, the higher or lower pH value would directly affect the activity of methanogens, and then the anaerobic digestion process in the reactor. The pH value of the influent and sludge mixture in the two systems was detected every day (Fig. 4a and 4b). Here the pH value of ScMFC-AnMBR always remained within the 7.09±0.06 range throughout the whole operational cycle, while the pH value in C-AnMBR was as low as 6.55 in the late operational period and acidification occurred. Therefore, the bioelectric field in ScMFC-AnMBR helped improve the anti-acidification performance.

When the MLVSS to MLSS ratio is higher than 0.85 or less than 0.4, it was indicated that the sludge does not appear under ideal conditions. MLSS and MLVSS of the two systems measured every 5 days are shown in Fig. 4c and 4d. The values of suspended solids in two systems were very close (MLSS and MLVSS in ScMFC-

AnMBR were only 3.9% and 3.2% higher than those in C-AnMBR, respectively) and presented relatively stable growth trends. It showed that the advantage of metabolic strains breeding and disadvantage of die cracking in the reactor were in a state of relative balance during the operation, which met the requirements of comparative analysis between the two systems. Meanwhile, the ratio of MLVSS to MLSS in both groups fluctuated around 0.6, indicating the activity of anaerobic sludge was always stable within the desired range.

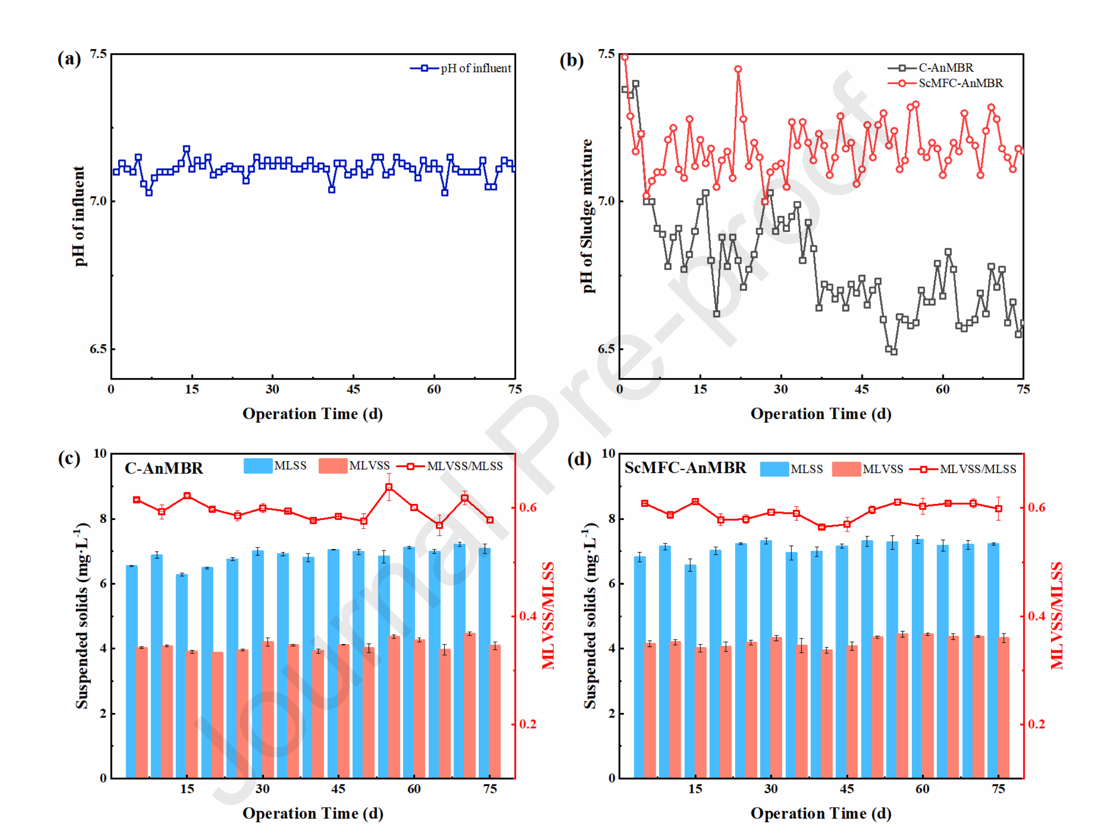

Fig. 4. (a) pH of influent, (b) pH of sludge mixture, suspended solids in C-AnMBR (c) and ScMFC-AnMBR (d) during operation time.

3.2.4 Membrane fouling and mitigation mechanism

As shown in Fig. 5a, the transmembrane pressure (TMP) in C-AnMBR grew slowly in the first four days. With the extension of running time, the TMP in C-AnMBR began to grow rapidly and exceeded 35 kPa on days 38, 56 and 73. Subsequently, chemical cleaning was carried out on the membrane components. In C-AnMBR, the operational cycle of the membrane component was gradually shortened when TMP reached 35 kPa again, which meant that the membrane fouling rate increased after cleaning. It was difficult to ensure the long-term stable operation of the membrane fouling control of C-AnMBR only by means of cleaning. This was related to the self-accelerating characteristics of membrane fouling. The removal of fouling by membrane cleaning was not complete. The remaining biofilms and EPS on the membrane can regenerate quickly and attach microorganisms easily, therefore the fouling of cleaned membrane was much faster than that of the fresh membrane [31]. However, the TMP of ScMFC-AnMBR was in a slow growth status during the whole continuous flow operational cycle. In the latter part of the experiment, the TMP value of ScMFC-AnMBR was only 18.513 kPa. This phenomenon of significantly reduced membrane fouling rate can be attributed to the fact that the bioelectric field strengthened the electrostatic repulsion between microorganisms and stripped the pollutants from the membrane surface, thus slowing down the membrane fouling.

SMP and EPS are the supporting structures of biofilm and activated sludge, and they are also the main membrane fouling substances [32]. The measured SMP and EPS of C-AnMBR and ScMFC-AnMBR are illustrated in Fig. 5a and 5b. The SMP and EPS in the two systems exhibited an upward trend, because the substrate degradation microorganisms could reach a state of dynamic balance with the endogenous respiratory microorganisms after adapting to the environment. Since excessive EPS would cause serious membrane fouling, and the SMP content was also positively correlated with the membrane fouling rate, the content of SMP and EPS in the two systems was compared [33, 34]. It was obvious that the content of SMP and EPS in ScMFC-AnMBR was lower significantly (65.3% and 43.1%, respectively) compared to C-AnMBR.

However, the SMPp/SMPc ratio of ScMFC-AnMBR was higher, which reached 3.711. More notably, the EPSp/EPSc ratio of ScMFC-AnMBR reached 3.72, 1.33 higher than that of C-AnMBR. According to previous research, it has been reported that a higher SMPp/SMPc ratio reduced the irreversible fouling of membrane components [35]. Although the ratio of protein to carbohydrate was higher in ScMFC-AnMBR, the rate of membrane fouling of the integrated system was obviously lower than that of C-AnMBR. The bioelectric field effectively alleviated membrane fouling by reducing the amount of substances, thus slowing down the rate of membrane flux reduction in

ScMFC-AnMBR. Moreover, the comprehensive effects caused by the bioelectric field, including particle size, sludge charge, SMP\EPS content and microbial community structure change, were likely to work together to complete the important task of preventing or minimizing membrane fouling in the system.

Zeta potential of sludge can characterize the charged property of sludge surface, which also reflects the stability of anaerobic sludge. According to the Derjaguin-Landau-Verweyand-Overbeek (DLVO) theory [36], an increase in the absolute value of zeta potential means a rise in the static charge on the sludge surface, which enlarges the electrostatic repulsion between sludge particles and makes it difficult for sludge particles to combine with each other. Conversely since the absolute value of zeta potential was low, the effect of sludge flocculation was very clear. The absolute values of zeta potential of the sludge in ScMFC-AnMBR and C-AnMBR were 18.3 and 27.9, respectively. The absolute value decrease of zeta potential in ScMFC-AnMBR indicated that the sludge mixture had a stronger agglomeration ability compared with C-AnMBR, which was caused by a significant decline in EPS content in this system [37]. Furthermore, the changes of sludge particle size distribution in the two systems are shown in Fig. 5d.

At the initial stage of the experiment, the sludge particles size and distribution in the two systems were basically the same. However, with the extension of operational time, the particle size of the two systems increased by 19.32 μm and 10.98 μm compared with the initial operation, respectively. The sludge particle size in ScMFC-AnMBR increased rapidly to 54.33 μm, while it was less than 50 μm (only 45.93 μm) in C-AnMBR. The particle size increase was more obvious when the zeta potential value was low in ScMFC-AnMBR. It was generally believed that when the sludge particle size was less than 50 μm, the small particles of sludge were more likely to form a dense cake layer on the membrane components [38]. Thus, it contributed to more serious membrane fouling in C-AnMBR. From the perspective of the change of sludge zeta potential and sludge particle size distribution, the aggregation of sludge particles caused by the bioelectric field did make a great contribution to alleviate membrane fouling.

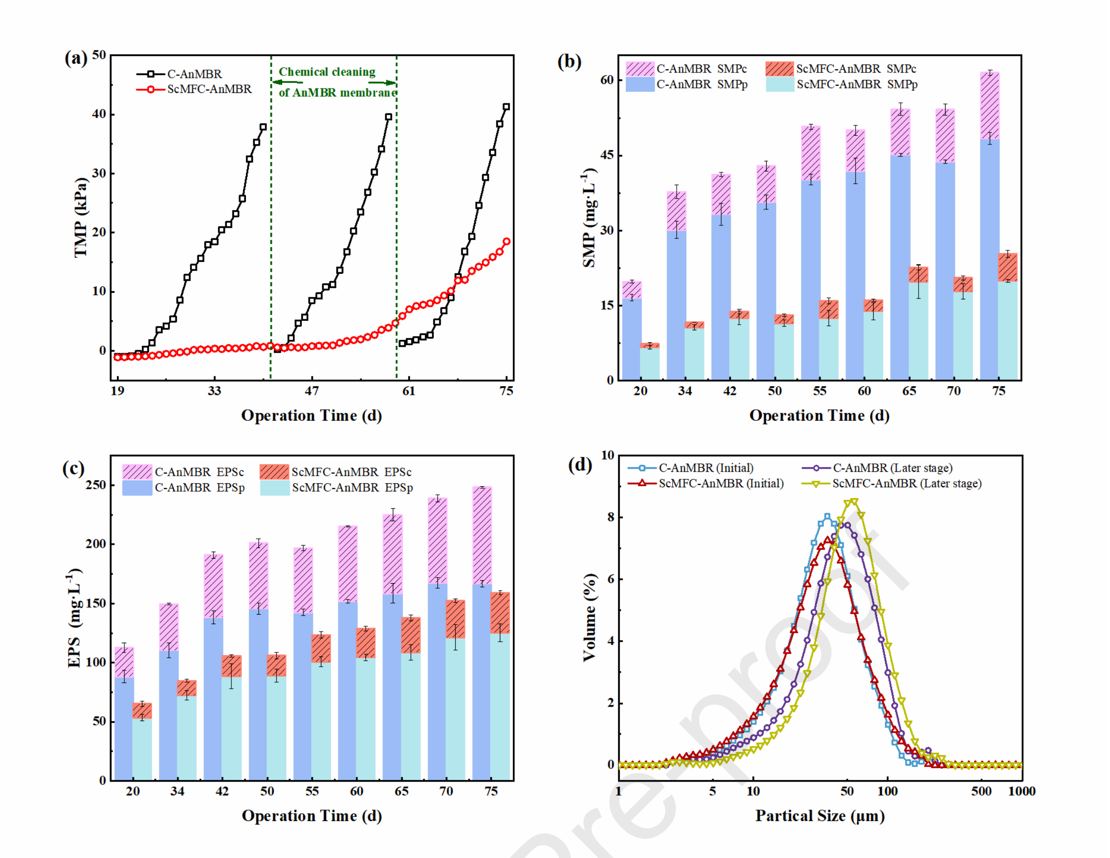

Fig. 5. (a) TMP variation of ScMFC-AnMBR and C-AnMBR，SMP and EPS in C-AnMBR (b) and ScMFC-AnMBR (c) during operation, (d) size distribution of activated sludge flocs in ScMFC-AnMBR and C-AnMBR; SMPc: carbohydrate in SMP; SMPp: proteins in SMP; EPSc: carbohydrate in EPS; EPSp: proteins in EPS.

The three-dimensional fluorescence spectra of SMP and EPS in C-AnMBR and ScMFC-AnMBR are illustrated in Fig. S2. The main peak was found in the range of $\lambda_{ex}/\lambda_{em}$ =210~230/330~360 nm and $\lambda_{ex}/\lambda_{em}$ =250~290/330~370 nm, representing common aromatic proteins or aromatic organic substances containing two to three benzene rings [39] and humic acids or organic substances containing three to five benzene rings [40], respectively. They showed strong persistence in the environment due to their difficult degradation [41]. Obviously, the existence of the bioelectric field weakened the fluorescence intensity of the EPS and SMP peaks in the reaction process, and the concentration of proteins and humic acids was significantly reduced, which agreed with what Wang, Bi, Ngo, Guo, Jia, Zhang and Zhang [6] reported. Under the influence of the bioelectric field, the deposition rate of substances causing membrane fouling diminished. Thus, the fouling of membrane components was slowed down to a certain extent and the operation cycle of the reactor was prolonged.

3.3 Microbial community diversity analysis

Through high-throughput sequencing analysis for the mixed sludge, the abundance of microorganisms was obtained in C-AnMBR and ScMFC-AnMBR. The top 20 abundances at phylum level of both systems are shown in Fig. 6a. Phylum Bacteroidetes (19%) of the two systems disappeared completely in Stage III. Although phylum Bacteroidetes was deemed to be an efficient bacterium for protein and carbohydrate degradation, they may not adapt to the influent components in this experiment. This was due to the feed composition and existing substrate concentration in the reactor possibly being more selective for microbial community composition than the composition of the raw sludge and reactor configuration [42]. The dominant bacteria of ScMFC-AnMBR in the latter part of Stage Ⅲ were phylum Firmicutes (16.04%), phylum Actinobacteria (29.02%), phylum Chloroflexi (5.02%) and phylum Desulfobacterota (14.01%), while the relative abundance in C-AnMBR were 31.81%, 13.79%, 8.34% and 5.06%, respectively. Interestingly, phylum Firmicutes constituted the main species of microorganisms in the initial start-up stage of MFC and can carry out extracellular electron transfer [43], but phylum Firmicutes were also a bio-foulant leading to membrane fouling [44]. The abundance of phylum Firmicutes in ScMFC-AnMBR was approximately 50% of that in C-AnMBR. It was indicated that the bioelectric field restricted the development of this bio-foulant, and phylum Firmicutes gradually became less.

Phylum Actinobacteria was considered to be an environmentally friendly strain that can be used for biological remediation [45], and its relative abundance in ScMFC-AnMBR was more than twice that of C-AnMBR, indicating that the bioelectric field promoted the growth of phylum Actinobacteria, and the complex synergistic effect among the bacteria in ScMFC-AnMBR helped to maintain the stability of the bioelectric field [46]. Compared with the raw sludge, the abundance of phylum Chloroflexi in ScMFC-AnMBR and C-AnMBR fell by 80.8% and 68.2%, respectively, so the presence of the bioelectric field caused the faster decline of phylum Chloroflexi abundance. Referring to SMP and EPS as the organic carbon sources of phylum Chloroflexi growth [47], the abundance of phylum Chloroflexi can characterize the content of SMP and EPS in the system. The reduction in phylum Chloroflexi abundance in ScMFC-AnMBR further indicated that the bioelectric field inhibited the secretions of SMP and EPS, thus alleviating membrane fouling. Phylum Desulfobacterota is an electricity generator with high electron transfer efficiency, and its abundance in ScMFC-AnMBR was enhanced [26], ensuring the stable operation of the bioelectric field.

The top 20 examples of abundance at the genus level of both systems are shown in Fig. 6b. The abundance levels of *Brooklawnia* (14.05%) and *Trichococcus* (4.51%) in ScMFC-AnMBR were 12.33% and 4.5%, respectively, higher than in C-AnMBR. *Brooklawnia* can take up VFAs as the main fermentation product and plays an important role in hydrolysis and acid production during anaerobic digestion [48]. At the same time, *Brooklawnia* is part of the phylum Actinobacteria species, and its high growth in ScMFC-AnMBR corresponded to elevated phylum Actinobacteria abundance, which may help the stable voltage output of the bioelectric field. *Trichococcus* can decompose complex organic matter into simple organic matter such as lactic acid, acetic acid, formic acid and ethanol, making it a favorable substrate for other bacteria and methanogens [49]. Additionally, the abundance of acidophilic bacteria *Desulfovibrio* in ScMFC-AnMBR amounted to 6.81% while in C-AnMBR it was 3.65%. All these indicated that the hydrolytic acidification process in ScMFC-AnMBR was smoother than that in C-AnMBR, thereby greatly improving the methanogenic performance of the AnMBR system. More notably, the relative abundance of *Megasphaera* in ScMFC-AnMBR was only 0.002%, while the abundance of that in C-AnMBR was 7.87%. The significant decrease in the relative abundance of *Megasphaera* (belonging to phylum Firmicutes) in ScMFC-AnMBR explained the decrease in the abundance of phylum Firmicutes. Since *Megasphaera* was a bio-foulant that easily adhered under acidic conditions [50], the reduction in *Megasphaera* meant that the bioelectric field environment inhibited the growth of bio-foulant and thus mitigated membrane fouling.

A comprehensive analysis of methanogens and exoelectrogens in the two systems reported that the relative abundance of methanogens and exoelectrogens in ScMFC-AnMBR was higher than that in C-AnMBR (Fig. 6c and 6d). Interestingly, hydrogenotrophic methanogens (*Methanobacterium*) were the dominant methanogens in C-AnMBR during the later stages of operation, with a relative abundance of 11%. Conversely, in ScMFC-AnMBR, the relative abundance of *Methanobacterium* diminished to 2.17%, and aceticlastic methanogens (*Methanosaeta*) emerged as the dominant methanogens, with a relative abundance of 6.83%. This outcome corresponded to the significant decrease of VFAs content in ScMFC-AnMBR, indicating that the system can better resist acidification. It was worth noting that *Syntrophobacter* and *Smithella* were the two major syntrophic bacteria of methanogens, and their abundances were positively correlated with methanogens [51]. Furthermore, *Syner-01* was deemed to be an acid fermentation bacterium, which further enhanced methanogenesis in a syntrophic way with *Methanosaeta* [52].

As a result, the relative abundance of the three bacteria in the two systems at the late part of Stage III was compared. It emerged that the abundance of *Syntrophobacter* (0.46%), *Smithella* (1.37%) and *Syner-01* (1.22%) in ScMFC-AnMBR was 8.9 times, 14.6 times and 305 times higher than that in C-AnMBR, respectively. Here, it is suggested that the bioelectric field enhanced methanogenic activity by increasing the abundance of syntrophic bacteria of methanogens, and then enabled ScMFC-AnMBR to perform better methanogenically. *Desulfovibrio* (6.81%) became the dominant exoelectrogens in ScMFC-AnMBR, and *Petrimonas* (0.93%), *Geobacter* (0.08%), *Bacillus* (0.42%) and *Thauera* (0.02%) also obtained a better breeding environment compared with C-AnMBR. There was a mutually beneficial relationship between MFC electricity generation and microbial enrichment and growth (Rabaey, Boon, Siciliano, Verhaege and Verstraete [53], so the stable bioelectric field in ScMFC-AnMBR was closely bound up with the synergistic effect of exoelectrogens. In the meantime, the stable bioelectric field environment promoted the reproduction and metabolism of exoelectrogens, putting into motion a virtuous cycle of electricity generation. To sum up, the stable micro-bioelectric field in ScMFC-AnMBR altered the structure of the microbial community, and strengthened the interaction between microorganisms.

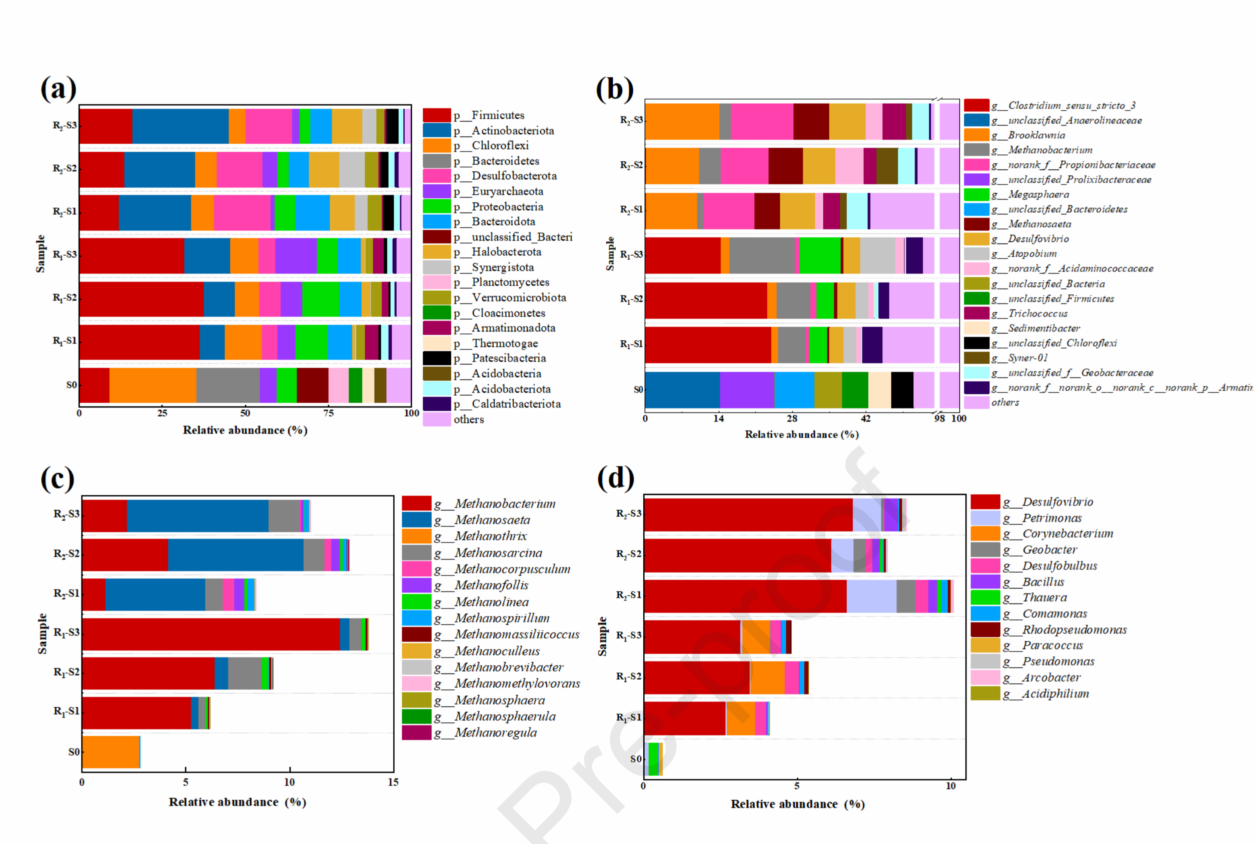

Fig. 6. Top 20 levels of abundance at (a) phylum and (b) genus level; (c) Relative abundance of methanogens and (d) exoelectrogens; R_1 and R_2 represent C-AnMBR and ScMFC-AnMBR, respectively. S0, S1, S2 and S3 represent raw sludge sample, sludge samples at the early, middle and late phase of Stage Ⅲ, respectively.

Table 1. Alpha diversity index in C-AnMBR (R_1) and ScMFC-AnMBR (R_2).

Sample	Sobs	Shannon	Simpson	Ace	Chao	Coverage
R_1-S1	1407	4.491487	0.064614	1655.879	1615.398	0.996971
R_1-S2	1331	4.402041	0.062412	1555.944	1521.048	0.997471
R_1-S3	1287	4.482407	0.038322	1526.732	1503.005	0.997612
R_2-S1	1152	4.510172	0.030007	1408.628	1369.775	0.997272
R_2-S2	1094	4.35349	0.032366	1305.507	1302.643	0.997484
R_2-S3	1025	4.092493	0.046227	1337.524	1302.44	0.997227

According to the Shannon index concerning the two systems (Table 1), their levels of microbial diversity were basically the same. In order to investigate changes in the structure of the microbial community due to the bioelectric field in ScMFC-AnMBR, principal component analysis (PCA) (Fig. S3) was conducted. Obviously, the separation distance of microorganisms in the two systems was large at PC1 and PC2 levels, but particularly at the PC1 level. These results indicated that the microbial relationship between the two systems was distant, and the existence of the bioelectric field did not improve the microbial diversity in ScMFC-AnMBR. Nonetheless, it significantly changed the structure of the microbial community. Based on these results, the microorganisms selected by the bioelectric field developed well and resulted in enhancing the AnMBR performance and minimizing the problem of membrane fouling.

The correlation network diagram between exoelectrogens and methanogens at the genus level is shown in Fig. 7, and reveals the interaction between two functional bacteria groups in ScMFC-AnMBR. The relative abundance of two acidophilic bacteria (*Desulfovibrio* (6.81%) *and Methanosaeta* (6.83%)) in ScMFC-AnMBR increased, which promoted the abundance of many methanogens (*Methanospirillum* (0.21%). *Methanofollis* (0.13%)) and exoelectrogens (*Bacillus*, *Petrimonas*, *Thauera*) which positively correlated with the two bacteria. Here the selected exoelectrogens and methanogens promoted each other in ScMFC-AnMBR, which did two things: ensure the stability of the bioelectric field; and promote anaerobic digestion in the system to a certain extent.

Meanwhile, *Methanosaeta* dominated the ScMFC-AnMBR system due to their greater affinity for acetic acid and lower threshold for acetic acid utilization [54]. The relative abundance of hydrogenotrophic methanogens (*Methanobacterium*, 2.17%) was only 17.5% of that of C-AnMBR, possibly the result of the electron transfer effect (combination of hydrogen and hydroxide ions) under the bioelectric field. It also led to better functional bacteria negatively related to *Methanobacterium*. These functional bacteria included exoelectrogens, mesophili methanogens (*Methanofollis*), hydrogenotrophic methanogens (*Methanospirillum*) and *Methanosarcina* (1.5%). De Vrieze, Hennebel, Boon and Verstraete [55] noted that *Methanosarcina* had a higher growth rate and tolerance than other methanogens, while Walter, Probst, Hinterberger, Muller and Insam [56] pointed out that *Methanosarcina* abundance did positively correlate with methanogenic performance. Therefore, the increase in *Methanosarcina* abundance in the bioelectric field environment strongly suggests that ScMFC-AnMBR performed excellently in the methanogenic scenario. In brief, the enhanced methanogenic performance of ScMFC-AnMBR did rely on the interaction between methanogens and exoelectrogens. Of these, *Desulfovibrio*, *Methanosaeta* and *Methanosarcina* contributed the most.

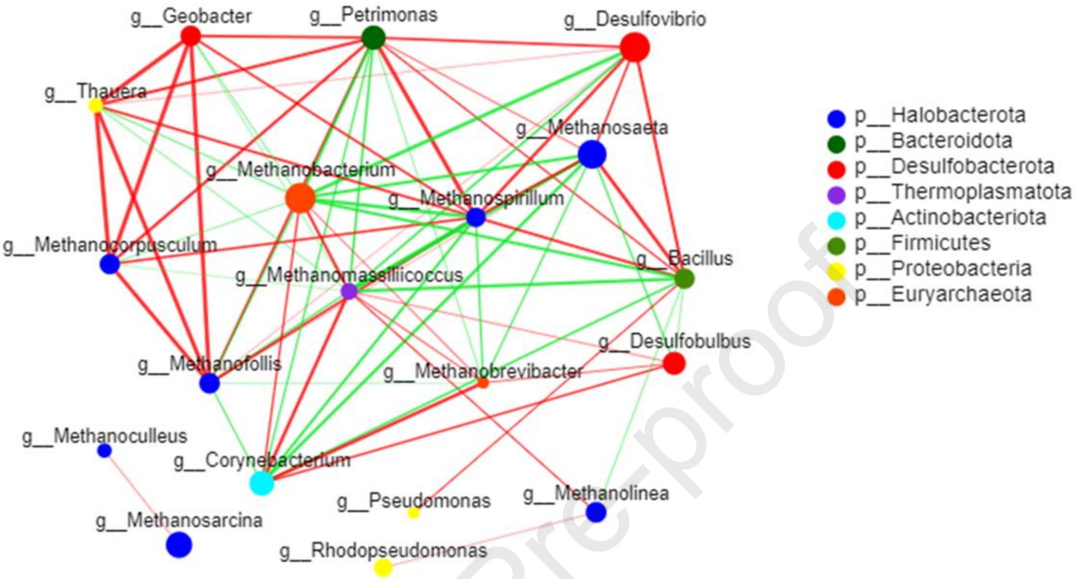

Fig. 7. Correlation network diagram between methanogens and electrogenic bacteria at genus level. (The node size represents species abundance, different colors represent species at different phylum levels, line color represents positive and negative correlation, red represents positive correlation, green represents negative correlation, thicker line indicates higher correlation between species, and more lines indicate a closer relationship between this species and other species.)

4. Conclusions

A novel ScMFC-AnMBR system, combining an AnMBR with a single-chamber air-cathode MFC, was constructed for the purposes of enhancing methane production and reducing membrane fouling. The ScMFC-AnMBR system provided a stable micro-bioelectric field under constant influent load. Compared with C-AnMBR, the COD removal and methane production using the ScMFC-AnMBR clearly improved, and superior acidizing resistance was obtained. Moreover, the comprehensive effects caused by the bioelectric field, including particle size, sludge charge, SMP\EPS content and microbial community structure change, jointly alleviated membrane fouling in the system. Furthermore, the abundance of aceticlastic methanogens (*Methanosaeta*), syntrophic bacteria of methanogens (*Syntrophobacter*, *Smithella* and *Syner-01*) and exoelectrogens with better electron transfer function (*Desulfovibrio*) increased., Meanwhile the abundance of bio-foulant (*Megasphaera*) decreased in the ScMFC-AnMBR system. The two functional microbes of exoelectrogens and methanogens helped each other, stabilizing the bioelectric field and enhancing the activity of methanogens. The integrated system significantly improved the methanogenic performance, shortened the start-up period, and alleviated membrane fouling under the stable micro-bioelectric field, emphasizing the feasibility of the ScMFC-AnMBR to treat wastewater efficiently and effectively.

Acknowledgements

This research was supported by Tianjin Municipal Science and Technology Bureau of China (Project No. 20JCZDJC00380, 21YDTPJC00660, and 18PTZWHZ00140).

References

[1] P. Krzeminski, L. Leverette, S. Malamis, E. Katsou, Membrane bioreactors - A review on recent developments in energy reduction, fouling control, novel configurations, LCA and market prospects, J. Membr. Sci. 527 (2017) 207-227. https://doi.org/10.1016/j.memsci.2016.12.010.

[2] C.W. Teo, P.C.Y. Wong, Enzyme augmentation of an anaerobic membrane bioreactor treating sewage containing organic particulates, Water Res. 48 (2014) 335-344. https://doi.org/10.1016/j.watres.2013.09.041.

[3] A. Yurtsever, E. Sahinkaya, O. Aktas, D. Ucar, O. Cinar, Z.W. Wang, Performances of anaerobic and aerobic membrane bioreactors for the treatment of synthetic textile wastewater, Bioresour. Technol. 192 (2015) 564-573. https://doi.org/10.1016/j.biortech.2015.06.024.

[4] L.G. Shen, Q. Lei, J.R. Chen, H.C. Hong, Y.M. He, H.J. Lin, Membrane fouling in a submerged membrane bioreactor: Impacts of floc size, Chem. Eng. J. 269 (2015) 328-334. https://doi.org/10.1016/j.cej.2015.02.002.

[5] G.Y. Zhen, Y. Pan, X.Q. Lu, Y.Y. Li, Z.Y. Zhang, C.X. Niu, G. Kumar, T. Kobayashi, Y.C. Zhao, K.Q. Xu, Anaerobic membrane bioreactor towards biowaste biorefinery and chemical energy harvest: Recent progress, membrane fouling and future perspectives, Renew. Sust. Energ. Rev. 115 (2019) 24. https://doi.org/10.1016/j.rser.2019.109392.

[6] J. Wang, F.H. Bi, H.H. Ngo, W.S. Guo, H. Jia, H.W. Zhang, X.B. Zhang, Evaluation of energy-distribution of a hybrid microbial fuel cell-membrane bioreactor (MFC-MBR) for cost-effective wastewater treatment, Bioresour. Technol. 200 (2016) 420-425. https://doi.org/10.1016/j.biortech.2015.10.042.

[7] K.P. Katuri, C.M. Werner, R.J. Jimenez-Sandoval, W. Chen, S. Jeon, B.E. Logan, Z.P. Lai, G.L. Arny, P.E. Saikaly, A novel anaerobic electrochemical membrane bioreactor (AnEMBR)

with conductive hollow-fiber membrane for treatment of low-organic strength solutions, Environ. Sci. Technol. 48(21) (2014) 12833-12841. https://doi.org/10.1021/es504392n.

[8] A.Q. Ding, Q. Fan, R. Cheng, G.D. Sun, M.J. Zhang, D.L. Wu, Impacts of applied voltage on microbial electrolysis cell-anaerobic membrane bioreactor (MEC-AnMBR) and its membrane fouling mitigation mechanism, Chem. Eng. J. 333 (2018) 630-635. https://doi.org/10.1016/j.cej.2017.09.190.

[9] Y. Yang, S. Qiao, R.F. Jin, J.T. Zhou, X. Quan, Fouling control mechanisms in filtrating natural organic matters by electro-enhanced carbon nanotubes hollow fiber membranes, J. Membr. Sci. 553 (2018) 54-62. https://doi.org/10.1016/j.memsci.2018.02.012.

[10] Y. Yang, S. Qiao, R.F. Jin, J.T. Zhou, X. Quan, Novel anaerobic electrochemical membrane bioreactor with a CNTs hollow fiber membrane cathode to mitigate membrane fouling and enhance energy recovery, Environ. Sci. Technol. 53(2) (2019) 1014-1021. https://doi.org/10.1021/acs.est.8b05186.

[11] S. Zhang, K. Yang, W. Liu, Y. Xu, S.Q. Hei, J. Zhang, C. Chen, X.Z. Zhu, P. Liang, X.Y. Zhang, X. Huang, Understanding the mechanism of membrane fouling suppression in electro-anaerobic membrane bioreactor, Chem. Eng. J. 418 (2021) 10. https://doi.org/10.1016/j.cej.2021.129384.

[12] Y. Tian, C. Ji, K. Wang, P. Le-Clech, Assessment of an anaerobic membrane bio-electrochemical reactor (AnMBER) for wastewater treatment and energy recovery, J. Membr. Sci. 450 (2014) 242-248. https://doi.org/10.1016/j.memsci.2013.09.013.

[13] J.D. Liu, C. Tian, X.L. Jia, J.X. Xiong, S.N. Dong, L. Wang, L.L. Bo, The brewery wastewater treatment and membrane fouling mitigation strategies in anaerobic baffled anaerobic/aerobic membrane bioreactor, Biochem. Eng. J. 127 (2017) 53-59. https://doi.org/10.1016/j.bej.2017.07.009.

[14] G. Yang, J. Wang, H.W. Zhang, H. Jia, Y. Zhang, F. Gao, Applying bio-electric field of microbial fuel cell-upflow anaerobic sludge blanket reactor catalyzed blast furnace dusting ash for promoting anaerobic digestion, Water Res. 149 (2019) 215-224. https://doi.org/10.1016/j.watres.2018.10.091.

[15] Y. Jeong, Y. Kim, Y. Jin, S. Hong, C. Park, Comparison of filtration and treatment performance between polymeric and ceramic membranes in anaerobic membrane bioreactor treatment of domestic wastewater, Sep. Purif. Technol. 199 (2018) 182-188. https://doi.org/10.1016/j.seppur.2018.01.057.

[16] S. Cheng, H. Liu, B.E. Logan, Increased performance of single-chamber microbial fuel cells using an improved cathode structure, Electrochemistry Communications 8(3) (2006) 489-494. https://doi.org/10.1016/j.elecom.2006.01.010.

[17] A.E. Greenberg, R.R. Trussell, L.S. Clesceri, A.W.W. Association, Standard methods for the examination of water and wastewater : supplement to the sixteenth edition, American Journal of Public Health & the Nations Health 56(3) (2005) 387. https://doi.org/10.2105/AJPH.56.4.684-a.

[18] Adriana, Ledezma, Estrada, Yuan, Liu, Guangyin, Zhen, Yu-You, Li, Toshimasa, Long-term effect of the antibiotic cefalexin on methane production during waste activated sludge anaerobic digestion, Bioresource Technology: Biomass, Bioenergy, Biowastes, Conversion Technologies, Biotransformations, Production Technologies 169 (2014) 644-651. https://doi.org/10.1016/j.biortech.2014.07.056.

[19] C. Chen, Y. Zhang, B. Zhang, X. Ma, Z. Liu, M. Cao, Y. Chai, F. Chen, Study on the

characteristics of microbial community in anaerobic fluidized bed membrane bioreactor for domestic wastewater treatment, Acta Scientiae Circumstantiae 39(7) (2019) 2099-2107. https://doi.org/10.13671/j.hjkxxb.2019.0041.

[20] M.A. Rodrigo, P. Canizares, J. Lobato, R. Paz, C. Saez, J.J. Linares, Production of electricity from the treatment of urban waste water using a microbial fuel cell, J. Power Sources 169(1) (2007) 198-204. https://doi.org/10.1016/j.jpowsour.2007.01.054.

[21] K.J. Chae, M.J. Choi, J.W. Lee, K.Y. Kim, I.S. Kim, Effect of different substrates on the performance, bacterial diversity, and bacterial viability in microbial fuel cells, Bioresour. Technol. 100(14) (2009) 3518-3525. https://doi.org/10.1016/j.biortech.2009.02.065.

[22] T. Sleutels, S.D. Molenaar, A. Ter Heijne, C.J.N. Buisman, Low substrate loading limits methanogenesis and leads to high coulombic efficiency in bioelectrochemical systems, Microorganisms 4(1) (2016) 11. https://doi.org/10.3390/microorganisms4010007.

[23] S. Jung, J.M. Regan, Comparison of anode bacterial communities and performance in microbial fuel cells with different electron donors, Appl. Microbiol. Biotechnol. 77(2) (2007) 393-402. https://doi.org/10.1007/s00253-007-1162-y.

[24] Z.Y. Ren, H.J. Yan, W. Wang, M.M. Mench, J.M. Regan, Characterization of microbial fuel cells at microbially and electrochemically meaningful time scales, Environ. Sci. Technol. 45(6) (2011) 2435-2441. https://doi.org/10.1021/es103115a.

[25] K. Fricke, F. Harnisch, U. Schroder, On the use of cyclic voltammetry for the study of anodic electron transfer in microbial fuel cells, Energy Environ. Sci. 1(1) (2008) 144-147. https://doi.org/10.1039/b802363h.

[26] N.N. Zhao, L. Treu, I. Angelidaki, Y.F. Zhang, Exoelectrogenic anaerobic granular sludge for simultaneous electricity generation and wastewater treatment, Environ. Sci. Technol. 53(20) (2019) 12130-12140. https://doi.org/10.1021/acs.est.9b03395.

[27] J.C. Thrash, J.D. Coates, Review: Direct and indirect electrical stimulation of microbial metabolism, Environ. Sci. Technol. 42(11) (2008) 3921-3931. https://doi.org/10.1021/es702668w.

[28] Q.D. Yin, K. He, A.K. Liu, G.X. Wu, Enhanced system performance by dosing ferroferric oxide during the anaerobic treatment of tryptone-based high-strength wastewater, Appl. Microbiol. Biotechnol. 101(9) (2017) 3929-3939. https://doi.org/10.1007/s00253-017-8194-8.

[29] K.C. Wijekoon, C. Visvanathan, A. Abeynayaka, Effect of organic loading rate on VFA production, organic matter removal and microbial activity of a two-stage thermophilic anaerobic membrane bioreactor, Bioresour. Technol. 102(9) (2011) 5353-5360. https://doi.org/10.1016/j.biortech.2010.12.081.

[30] C. Chernicharo, Post-treatment options for the anaerobic treatment of domestic wastewater, Reviews in Environmental Science and Bio/Technology 5(1) (2006) 73-92. https://doi.org/10.1007/s11157-005-5683-5.

[31] P. Le-Clech, V. Chen, T. Fane, Fouling in membrane bioreactors used in wastewater treatment, J. Membr. Sci. 284(1-2) (2006) 17-53. https://doi.org/10.1016/j.memsci.2006.08.019.

[32] A. Deb, K. Gurung, J. Rumky, M. Sillanpaa, M. Manttari, M. Kallioinen, Dynamics of microbial community and their effects on membrane fouling in an anoxic-oxic gravity-driven membrane bioreactor under varying solid retention time: A pilot-scale study, Sci Total Environ 807(Pt 2) (2022) 150878. https://doi.org/10.1016/j.scitotenv.2021.150878.

[33] T. Yu, L. Chen, S. Zhang, C. Cao, S. Zhang, Correlating membrane fouling with sludge characteristics in membrane bioreactors: An especial interest in EPS and sludge morphology

analysis, Bioresour. Technol. 102(19) (2011) 8820-8827. https://doi.org/10.1016/j.biortech.2011.07.010.

[34] X. Zhang, X. Yue, Z. Liu, Q. Li, X. Hua, Impacts of sludge retention time on sludge characteristics and membrane fouling in a submerged anaerobic-oxic membrane bioreactor, Appl Microbiol Biotechnol 99(11) (2015) 4893-903. https://doi.org/10.1007/s00253-015-6383-x.

[35] M. Yao, B. Ladewig, K. Zhang, Identification of the change of soluble microbial products on membrane fouling in membrane bioreactor (MBR), Desalination 278(1-3) (2011) 126-131. https://doi.org/10.1016/j.desal.2011.05.012.

[36] Yu, Yuexian, Ma, Liqiang, Xu, Hongxiang, Sun, Xianfeng, Zhang, Zhijun, DLVO theoretical analyses between montmorillonite and fine coal under different pH and divalent cations, Powder Technology An International Journal on the Science & Technology of Wet & Dry Particulate Systems (2018). https://doi.org/10.1016/j.powtec.2018.02.016.

[37] F. Meng, H. Zhang, F. Yang, S. Zhang, Y. Li, X. Zhang, Identification of activated sludge properties affecting membrane fouling in submerged membrane bioreactors, Sep. Purif. Technol. 51(1) (2006) 95-103. https://doi.org/10.1016/j.seppur.2006.01.002.

[38] R. Bai, H.F. Leow, Microfiltration of activated sludge wastewater—the effect of system operation parameters, Separation & Purification Technology 29(2) (2002) 189-198. https://doi.org/10.1016/s1383-5866(02)00075-8.

[39] P.J. He, Z. Zheng, H. Zhang, L.M. Shao, Q.Y. Tang, PAEs and BPA removal in landfill leachate with Fenton process and its relationship with leachate DOM composition, Sci. Total Environ. 407(17) (2009) 4928-4933. https://doi.org/10.1016/j.scitotenv.2009.05.036.

[40] R.D. Jiji, G.A. Cooper, K.S. Booksh, Excitation-emission matrix fluorescence based determination of carbamate pesticides and polycyclic aromatic hydrocarbons, Anal. Chim. Acta 397(1-3) (1999) 61-72. https://doi.org/10.1016/s0003-2670(99)00392-x.

[41] W. Chen, P. Westerhoff, J.A. Leenheer, K. Booksh, Fluorescence excitation - Emission matrix regional integration to quantify spectra for dissolved organic matter, Environ. Sci. Technol. 37(24) (2003) 5701-5710. https://doi.org/10.1021/es034354c.

[42] H. Park, A. Rosenthal, R. Jezek, K. Ramalingam, J. Fillos, K. Chandran, Impact of inocula and growth mode on the molecular microbial ecology of anaerobic ammonia oxidation (anammox) bioreactor communities, Water Res 44(17) (2010) 5005-13. https://doi.org/10.1016/j.watres.2010.07.022.

[43] S.H. Zhang, C.H. Qiu, C.F. Fang, Q.L. Ge, Y.X. Hui, B. Han, S. Pang, Characterization of bacterial communities in anode microbial fuel cells fed with glucose, propyl alcohol and methanol, Appl. Biochem. Microbiol. 53(2) (2017) 250-257. https://doi.org/10.1134/s0003683817020193.

[44] H. Fakhri, D.N. Arabaci, I.D. Unlu, C. Yangin-Gomec, S. Ovez, S. Aydin, Addition of trichocladium canadense to an anaerobic membrane bioreactor: evaluation of the microbial composition and reactor performance, Biofouling 37(7) (2021) 711-723. https://doi.org/10.1080/08927014.2021.1949002.

[45] A. Alvarez, J.M. Saez, J.S. Davila Costa, V.L. Colin, M.S. Fuentes, S.A. Cuozzo, C.S. Benimeli, M.A. Polti, M.J. Amoroso, Actinobacteria: Current research and perspectives for bioremediation of pesticides and heavy metals, Chemosphere 166 (2017) 41-62. https://doi.org/10.1016/j.chemosphere.2016.09.070.

[46] B. Hou, R. Zhang, X. Liu, Y. Li, P. Liu, J. Lu, Study of membrane fouling mechanism during the phenol degradation in microbial fuel cell and membrane bioreactor coupling system,

Bioresour Technol 338 (2021) 125504. https://doi.org/10.1016/j.biortech.2021.125504.

[47] Z.-r. Chu, K. Wang, X.-k. Li, M.-t. Zhu, L. Yang, J. Zhang, Microbial characterization of aggregates within a one-stage nitritation–anammox system using high-throughput amplicon sequencing, Chem. Eng. J. 262 (2015) 41-48. https://doi.org/10.1016/j.cej.2014.09.067.

[48] Y. Kim, S. Li, L. Chekli, S. Phuntsho, N. Ghaffour, T. Leiknes, H.K. Shon, Influence of fertilizer draw solution properties on the process performance and microbial community structure in a side-stream anaerobic fertilizer-drawn forward osmosis - ultrafiltration bioreactor, Bioresour. Technol. 240 (2017) 149-156. https://doi.org/10.1016/j.biortech.2017.02.098.

[49] T.W. Hao, L. Wei, H. Lu, H.K. Chui, H.R. Mackey, M.C.M. van Loosdrecht, G.H. Chen, Characterization of sulfate-reducing granular sludge in the SANI (R) process, Water Res. 47(19) (2013) 7042-7052. https://doi.org/10.1016/j.watres.2013.07.052.

[50] M. Bittner, J. Strejc, D. Matoulkova, Z. Kolska, L. Pustelnikova, T. Branyik, Adhesion of Megasphaera cerevisiaeonto solid surfaces mimicking materials used in breweries, Journal of the Institute of Brewing 123(2) (2017) 204-210. https://doi.org/10.1002/jib.415.

[51] Q. Du, Q.H. Mu, G.X. Wu, Metagenomic and bioanalytical insights into quorum sensing of methanogens in anaerobic digestion systems with or without the addition of conductive filter, Sci. Total Environ. 763 (2021) 10. https://doi.org/10.1016/j.scitotenv.2020.144509.

[52] K. Ma, W. Wang, Y. Liu, L. Bao, Y. Cui, W. Kang, Q. Wu, X. Xin, Insight into the performance and microbial community profiles of magnetite-amended anaerobic digestion: Varying promotion effects at increased loads, Bioresour Technol 329 (2021) 124928. https://doi.org/10.1016/j.biortech.2021.124928.

[53] K. Rabaey, N. Boon, S.D. Siciliano, M. Verhaege, W. Verstraete, Biofuel cells select for microbial consortia that self-mediate electron transfer, Appl. Environ. Microbiol. 70(9) (2004) 5373-5382. https://doi.org/10.1128/aem.70.9.5373-5382.2004.

[54] T.W. Song, S.S. Li, W.D. Ding, H.S. Li, M.T. Bao, Y. Li, Biodegradation of hydrolyzed polyacrylamide by the combined expanded granular sludge bed reactor-aerobic biofilm reactor biosystem and key microorganisms involved in this bioprocess, Bioresour. Technol. 263 (2018) 153-162. https://doi.org/10.1016/j.biortech.2018.04.121.

[55] J. De Vrieze, T. Hennebel, N. Boon, W. Verstraete, Methanosarcina: The rediscovered methanogen for heavy duty biomethanation, Bioresour. Technol. 112 (2012) 1-9. https://doi.org/10.1016/j.biortech.2012.02.079.

[56] A. Walter, M. Probst, S. Hinterberger, H. Muller, H. Insam, Biotic and abiotic dynamics of a high solid-state anaerobic digestion box-type container system, Waste Manage. 49 (2016) 26-35. https://doi.org/10.1016/j.wasman.2016.01.039.